Comparisons of Infrared Colors and Emission-line Intensities between Two types of Seyfert 2 Galaxies

Lin-Peng Cheng[⋆], Yong-Heng Zhao and Jian-Yan Wei

National Astronomical Observatories, Chinese Academy of Sciences, Beijing 100012

Abstract   We study the relation between the infrared colors, [OIII] emission lines, gaseous absorbing column density ($N_{\rm H}$),and the detectability of the polarized (hidden) broad-line region (HBLR) in a large sample of 75 Seyfert 2 galaxies (Sy2s). From the indicators of star-formation activity, f_{60}/f_{100} and $L_{\rm FIR}/L_{\rm B}$, we find some evidence that the Sy2s without HBLR show higher star-formation activities than those with HBLR, in agreement with previous prediction. Also, we confirm that the HBLR Sy2s tend to have a larger luminosity ratio of the core to the host galaxy, suggesting that the HBLR Sy2s display more powerful AGN activity. However, the level of obscuration found in previous papers is nearly indistinguishable between the two types of Sy2s. The results support the statement that the non-HBLR Sy2s, with a weaker core component and a stronger star-formation activity component, are intrinsically different from the HBLR Sy2s, which are Sy1 systems with a hidden powerful AGN core and a low star-formation activity. The indications are that the non-HBLR Sy2s might be at an earlier evolutionary phase than the HBLR Sy2s.

Key words: galaxies: active – galaxies: Seyfert – polarization – star formation

1   INTRODUCTION

The unification model for Seyfert galaxies proposes that Seyfert 1 and 2 galaxies (Sy1s and Sy2s hereafter) are intrinsically the same objects, and the presence of an optically thick structure obscures the broad-line region (BLR) in Sy2s (Véron-Cetty & Véron 2000a). The most convincing evidence is the detection of polarized broad emission lines in some Seyfert 2 galaxies (Antonucci & Miller 1985; Tran 1995; Moran et al. 2000). Other strong support has come from hard X-ray, near-IR and mid-IR observations (e.g., Turner et al. 1997; Risaliti, Maiolino & Salvati 1999; Alonso-Herrero, Ward & Kotilainen 1997; Clavel et al. 2000) which showed that Sy2s are generally characterised by strong absorption whilst Sy1s are relatively unabsorbed. The optical spectropolarimetric observations of different samples of Seyfert 2s indicate that only about 40% of Sy2s show broad lines in their polarized spectra (e.g., Heisler et al. 1997;

⋆ E-mail: linpeng@astro.as.utexas.edu

Moran et al. 2000), although such surveys are probably biased since the pre-selection was done according to the broad-band polarization.

Initially, Heisler, Lumsden and Bailey (1997, hereafter HLB) suggested that the detectability of a hidden broad-line region (HBLR) is related to the inclination of the torus which, in turn, determines the $60\,\mu$m to $25\,\mu$m flux ratio. They found only galaxies with warm IRAS colors ($f_{60}/f_{25} < 4.0$) have a hidden BLR. Both of the Seyfert 2 types were found to be well matched in terms of redshift, overall polarization and detection rate of compact nuclear radio emission. Thus, they proposed that the IRAS f_{60}/f_{25} ratio provides a measure of the inclination of the torus to the line of sight: in those Sy2s with a cool IRAS color the torus is so highly inclined that even the broad line scattering screen is obscured, leading to the appearance of the non-HBLR Sy2s. When the torus is observed close to face-on, the HBLR should be easier to detect and the IR color should be hotter since we are observing the hotter dust emitting region, and this is what is observed.

More recently, however, several authors compared the absorbing column density inferred from the hard X-ray with the detectability of HBLR and found no correlation between the two. This result is in contrast to the HLB model (1997), which predicts a higher absorbing column for the non-HBLR Sy2s. Thus, Alexander, Lumsden and Gu suggested that the detectability of HBLR is mainly determined by the relative luminosity of the active core to the host galaxy (Alexander 2001; Lumsden et al. 2001; Gu et al. 2001). More contribution from the host galaxy would make the IR colors cooler and also dilute the nuclear optical spectrum, this makes it more difficult to detect the scattered polarized light, though over a small area the obscuring column density towards the nucleus also plays a role. On the other hand, Tran (2001) accounted for the non-detectability of HBLR with the the Sy1 nucleus being weak or absent. Thus, it is evident that the model of simple purely orientation-based unification is not applicable to all Seyfert galaxies. The simple model of the obscuring torus has been subject to some modification. Especially, while the pc-scale torus is most probably responsible for the huge absorbing columns ($N_{\rm H} > 10^{24}{\rm cm}^{-2}$) observed in several Sy2s, observational evidence was also found for a larger scale ($\sim 100\,{\rm pc}$) obscuring region with a lower absorbing column density ($N_{\rm H} \sim 10^{22}{\rm cm}^{-2}$, Granato et al. 1997; Matt 2000 and reference therein).

In this paper, we extend the work of Lumsden et al. (2001) to larger samples of Seyfert 2 galaxies, for which data of [OIII]$\lambda5007$Å line emission, absorbing $N_{\rm H}$ and the detection of HBLR are available. In addition, we try to check the evidence for the relatively strong star-formation activity in the non-HBLR sy2s by comparing the far-IR colors and the luminosity ratio, with the mid-IR colors, and by examining the radio−FIR relation.

2   THE SAMPLES

We collected the spectropolarimetric and other data from recent literature, and obtained a sample of 38 Seyfert 2 galaxies with HBLR and one of 37 Sy2s with no HBLR detections. The data for the two samples are presented in Tables 1 and 2, respectively. The Tables list, in turn, the name of the galaxy (column 1); the column density ($N_{\rm H}$) taken from Bassani et al. (1999), Rosaliti et al. (1999), Alexander (2001), Awaki (2000) and Tran (2001) (column 2); the infrared colors, f_{25}/f_{60} and f_{60}/f_{100}, (columns 3 and 4), taken from NED, Strauss et al. (1990), and IRAS FSC; the flux between 42.5 and 122.5 μm, FIR, where FIR $= 1.26 \times 10^{-14}(2.58 \times f_{60\mu{\rm m}} + f_{100\mu{\rm m}})$, (column 5); the radio 20cm flux density S_{20} (in mJy) (column 6), drawn mainly from NED, Tran (2001), and Gu et al. (2001); the emission ratio of [OIII]$\lambda5007$Å to

Hβ (R_{5007}) and the Equivalent Width of [OIII]λ5007Å (EW$_{5007}$) (columns 7 and 8), and the luminosity ratio $L_{\mathrm{FIR}}/L_{\mathrm{B}}$ drawn from refs. [1]–[6] (column 9).

we calculate the luminosity ratio of L_{FIR} to L_{B} according to the formula: $\log(L_{\mathrm{FIR}}/L_{\mathrm{B}}) = \log L_{\mathrm{FIR}} + 0.4\,M_{\mathrm{B}} + \mathrm{const.}(= 0.0)$. The redshift and absolute magnitude M_{B} are taken from Véron (2000)'s AGN catalogue, and the far-IR luminosity L_{FIR} is calculated asssuming $H_0 = 70\,\mathrm{km\,s^{-1}\,Mpc^{-1}}$, $q_0 = 0$.

Table 1　　Basic Data for the HBLR Seyfert 2 Galaxies

Name	N_{H} [a]	f_{25}/f_{60}	f_{60}/f_{100}	FIR [b]	S_{20} [c]	$\log R_{5007}$	EW$_{5007}$ [d]	$\log(L_{\mathrm{FIR}}/L_{\mathrm{B}})$
Circinus	43 000			12.07		1.07 [4]		
ESO 434−G40	162				14.6	0.98 [4]		
F05189−2524	490	0.251	1.114	0.611	29.1	1.05 [1]	45.3	36.69
F09104+4109	24	0.717		0.030		1.07 [4]	1084	36.37
F13197−1627	7943	0.485	1.077	0.261	275.3	1.28 [2]		
F20460+1925	250	0.602		0.024	18.9	0.78 [4]		36.10
F23060+0505	840	0.374	1.386	0.048	6.8	0.97 [2]		36.25
IC 3639	>100 000	0.3	0.703	0.38		0.91 [1]	110	35.98
IC 5063	2400	0.7	1.36	0.24		1.02 [1]	171	
MARK 3	11 000	0.756	1.172	0.17	1100	1.08 [4]	930 [5]	35.80
MARK 348	1060	0.643	0.83	0.061	281.5	1.02 [4]	190 [5]	35.75
MARK 463E	1600	0.725	1.135	0.095	376	0.83 [4]	50 [5]	35.73
MARK 477	>10 000	0.389	0.708	0.066	60.8	0.95 [4]	220 [5]	35.97
MARK 1210	>10 000	1.1	1.454	0.078	115			35.48
NGC 1068	>100 000	0.483	0.786	8.544	4845	1.07 [1]	460	36.37
NGC 2110	289	0.203	0.727	0.206	299	0.70 [4]	96 [5]	36.00
NGC 2273	>100 000	0.226	0.602	0.322	63.4	1.0 [4]	84 [6]	
NGC 3081	6600				5.7	1.19 [4]		
NGC 4388	4200	0.344	0.567	0.553	118.5	1.05 [1]	908	36.39
NGC 4507	2920	0.308		0.219	67.4	0.98 [4]		35.90
NGC 5506	340	0.48	0.947	0.388	355	0.92 [4]	480 [5]	36.44
NGC 7674	>100 000	0.348	0.676	0.278	220	1.01 [1]	584	36.28
WAS 49B	170	0.682						35.23
NGC 788			0.864	0.041		1.0 [4]		
NGC 591		0.226	0.57	0.109		1.0 [4]	190 [5]	
F00521−7054		0.784			17.5	0.90 [2]		36.33
F01475−0740		0.8	1.615	0.042	319	0.72 [2]		36.12
F02581−1136		0.941		0.034	9.0	1.19 [2]	8.0 [5]	
F04385−0828		0.585	1.095	0.122	17.4			
F15480−0344		0.682		0.086	42.2	1.36 [2]	140 [5]	
F22017+0319	5000	0.621	1.137	0.051	18.3	.97 [2]		35.60
MCG −3−34−64	7600	0.485	1.077	0.261	252	1.06 [1]	191	35.75
MCG −3−58−7		0.331	0.720	0.121	12.7			36.09
NGC 424	>10 000	0.967	0.989	0.081	23.3	0.7 [4]		35.67
NGC 513		0.144	0.479	0.114	53.7			35.18
NGC 5995		0.236	0.559	0.201	30.7	0.80 [1]	19.6	35.93
NGC 6552	6000	0.459	0.911	0.114	34.3			35.63
NGC 7682		0.468			61			

[a] Absorbing column density in units of 10^{20} cm^{-2}; [b] In units of 10^{-12} W m^{-2}; [c] In units of mJy; [d] the equivalent width of the 5007Å [OIII] line in −Å; [1] Lumsden et al. 2001; [2] de Grijp et al. 1992; [3] Goncalves et al. 1999; [4] Whittle 1992; [5] Dahari et al. 1988; [6] Ho et al. 1997.

Table 2   Basic Data for the non-HBLR Seyfert 2 Galaxies

Name	N_H a	f_{25}/f_{60}	f_{60}/f_{100}	FIR[b]	S_{20}[c]	$\log R_{5007}$	EW$_{5007}^d$	$\log(L_{FIR}/L_B)$
F19254–7245	1995	0.226	0.946	0.251	50	0.60 [1]	56.5	37.10
MARK 1066	>10 000	0.224	0.833	0.482		0.64 [3]	89 [5]	36.32
NGC 1143	>100	0.115	0.44	0.309	146	1.17 [1]	34.7	36.40
NGC 1386	>100 000	0.279	0.555	0.301	37.8	1.17 [4]		35.76
NGC 1667	>10 000	0.113	0.39	0.395	77.3	0.88 [6]	37	35.82
NGC 3281	7980	0.383	0.913	0.318	80.9	1.04 [4]		36.34
NGC 3393	>100 000	0.333	0.581	0.122	81.5			35.76
NGC 4941	4500	0.384	0.329	0.098	20.3			35.02
NGC 5128	2250	0.127	0.452	9.839				37.55
NGC 5135	>10 000	0.142	0.591	0.910	191.6	0.82 [1]	82.7	36.30
NGC 5347	>10 000	0.674	0.538	0.079	6.4	0.71 [4]		35.06
NGC 5643	>100 000	1.872	0.510	0.112		1.22 [4]		35.64
NGC 7130	>10 000	0.129	0.651	0.877	190.6	0.78 [1]	95.4	
NGC 7172	861	0.137	0.475	0.346	29.9	0.68 [1]	7.6	36.18
NGC 7496	501	0.189	0.544	0.471		0.56 [4]		36.23
NGC 7582	1240	0.131	0.674	2.515	166.0	0.35 [1]	34.8	36.96
NGC 7590	<9.2	0.120		0.467				36.30
NGC 5256	>100 000	0.144	0.679	0.371		0.67 [1]	101.1	36.01
MARK 1361		0.256	0.879	0.154		0.70 [1]	80	36.06
F00198–7926	>10 000	0.371	1.080	0.137	5.4	0.47 [1]	30.7	36.79
F03362–1642		0.472			9.3	0.79 [2]		36.60
M51	7500	0.161	0.372	7.214	430.9			
MARK 573		0.685	0.867	0.058	20.5	1.09 [4]	340 [5]	35.50
MARK 938	1000	0.145	0.959	0.749	67.5	0.6 [3]		36.27
NGC 1144	100	0.119	0.469	0.315	146	1.11 [5]	24	36.41
NGC 1241		0.137			168			
NGC 1320		0.498	0.782	0.179	6.5	1.0 [4]		
NGC 3079	160	0.051	0.50	2.571	608	0.62 [6]	3.5 [6]	36.37
NGC 3362		0.164			15.2			
NGC 3660		0.118	0.412	0.118	14.8			35.95
NGC 3982		0.124	0.427	0.432	50.1	1.33 [6]	152 [6]	35.07
NGC 4501		0.093	0.25	1.135	289	0.73 [6]	12 [6]	36.54
NGC 5283		0.619			12.8	1.09 [4]		
NGC 5695		0.228	0.318	0.041	6.6	1.07 [5]	26	
NGC 5929		0.177	0.668	0.470	100	0.59 [1]	59	36.04
NGC 6890		0.168	0.473	0.228	10	1.32 [4]		36.12
UGC 6100		0.351	0.380	0.037	10.5			34.96

[a] Absorbing column density in units of 10^{20} cm^{-2}; [b] In units of 10^{-12} W m^{-2}; [c] In units of mJy; [d] the equivalent width of the 5007Å [OIII] line in −Å; [1] Lumsden et al. 2001; [2] de Grijp et al. 1992; [3] Goncalves et al. 1999; [4] Whittle 1992; [5] Dahari et al. 1988; [6] Ho et al. 1997.

3   RESULTS OF COMPARING HBLR WITH NON-HBLR SEYFERT 2S

3.1 f_{60}/f_{100} and L_{FIR}/L_B versus f_{25}/f_{60}

Figure 1 shows a plot of the two indicators of the relative power of AGNs: f_{60}/f_{100} vs. f_{25}/f_{60}. The first is the cool far-IR emission, believed to arise mostly from circumnuclear

starbursts and star-formation activities (Hunt & Malkan 1999). The second measures the contribution of the mid-IR emission (f_{25}), known to come mostly from surrounding dust (e.g., torus) heated by AGNs (Rodriguez & Pèrez 1997). A t test shows that the distributions of f_{60}/f_{100} for the HBLRs and non-HBLRs are different at the 99.9% level, with the HBLR Sy2s occupying a distinct region of the plot from that occupied by the non-HBLR Sy2s. The HBLR Sy2s tend to show higher f_{25}/f_{60} and lower f_{60}/f_{100} ratios in the sense that they exhibit a stronger AGN and weaker star-formation activity. This evidently marks them as truly energetic AGNs, containing a Sy1 nucleus.
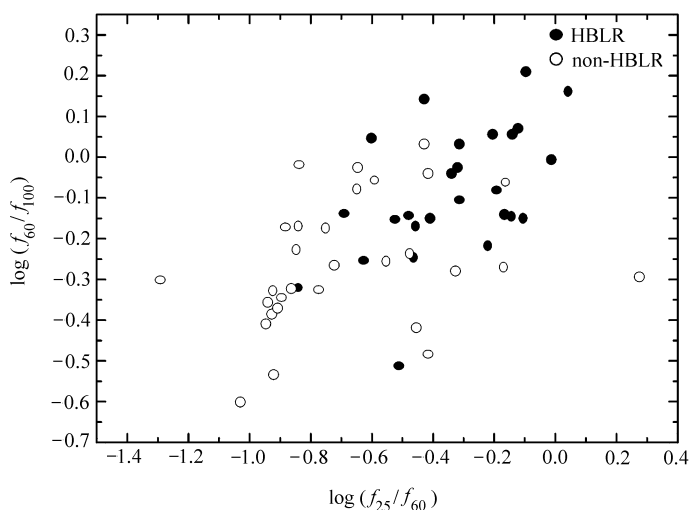
Fig. 1   IRAS color-color plot: f_{60}/f_{100} versus f_{25}/f_{60}. The HBLR Sy2s are shown as filled circles, and the non-HBLR Sy2s as open circles. The symbols in the following plots have the same coding.
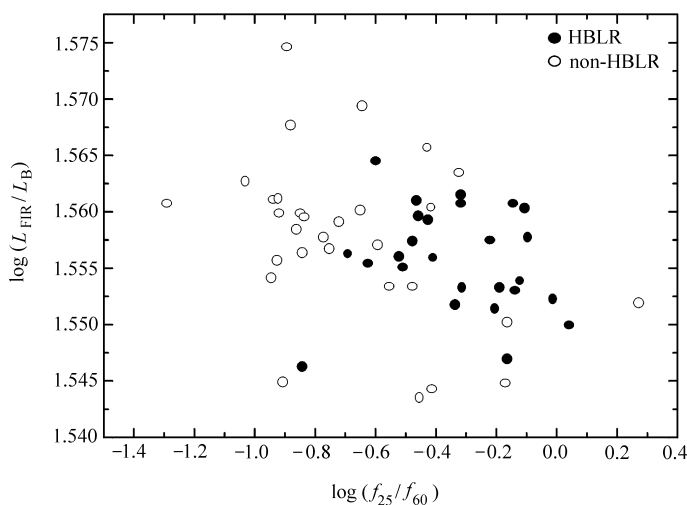
Fig. 2   Luminosity ratio of $L_{\mathrm{FIR}}/L_{\mathrm{B}}$ versus IR color f_{25}/f_{60} for the two types of Sy2s.

Figure 2 shows the $L_{\rm FIR}/L_{\rm B}$ versus f_{25}/f_{60} plot, which is used as an index of star-formation activity in galaxies (Keel 1993; Huang et al. 1996; Hunt & Malkan 1999). There is evidence that the HBLR and non-BHLR Sy2s are statistically segregated here, and that the latter display slightly higher $L_{\rm FIR}/L_{\rm B}$ at the 72.5% significance level. This result may be considered to be consistent with Figure 1: the non-HBLR Sy2s most probably are more active in star formation than the HBLR Sy2s.

3.2 [OIII]λ5007Å Emission Intensity and FIR/S_{20} versus f_{25}/f_{60}

Figure 3 shows a plot of the line ratio of [OIII]λ5007Å to Hβ (R_{5007}), which can serve as an indicator of the ionization level, versus f_{25}/f_{60}. A t test shows that the distributions of R_{5007} for the HBLRs and non-HBLRs are different at the 97% level. As can be seen, there is a tendency for higher ionization and warmer Sy2s to display HBLR indicative of a "buried Sy1 nucleus", a tendency noted earlier by Tran (1999), Alexander (2001), and Lumsden (2001). Assuming that both the warm and cool Sy2s have the same basic Seyfert 1 nucleus and galactic emission, the lower average emission line ratio in the non-HBLR Sy2s implies a larger ratio of galactic/star-formation to Seyfert activity (Alexander 2001).
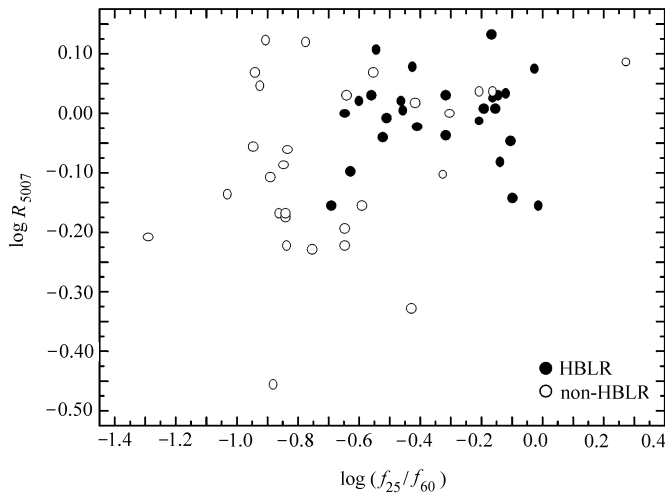
Fig. 3   Observed correlation between the intensity ratio of [OIII] λ5007Å to Hβ emission (R_{5007}) and IR color f_{25}/f_{60}.

Moreover, in Figures 4 and 5 we plot EW$_{5007}$ and FIR/S_{20} versus f_{25}/f_{60}. Compared to Fig. 3, the separation is more apparent at the same significance level, with the non-HBLR Sy2s showing smaller EW$_{5007}$ and higher FIR/S_{20}. The results are consistent with what was found by Lumsdens et al. (2001) for a smaller sample. Since EW$_{5007}$, as well as the FIR-radio flux ratio FIR/S_{20} (Gu et al. 2001), is widely used to measure the ratio of the luminosities in the active core and the host galaxy, the indications in Figures 4 and 5 are that the non-HBLR Sy2s have a weaker active core relative to the host galaxy.
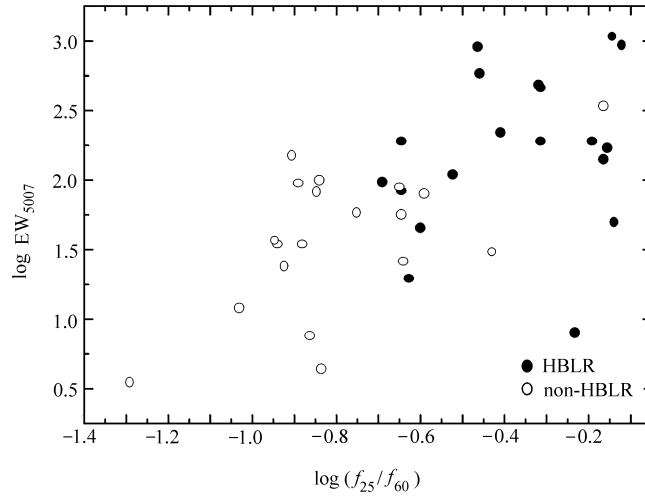
Fig. 4　Observed correlation between the equivalent width of [OIII] $\lambda5007$ Å (EW_{5007}) and IR color f_{25}/f_{60}.
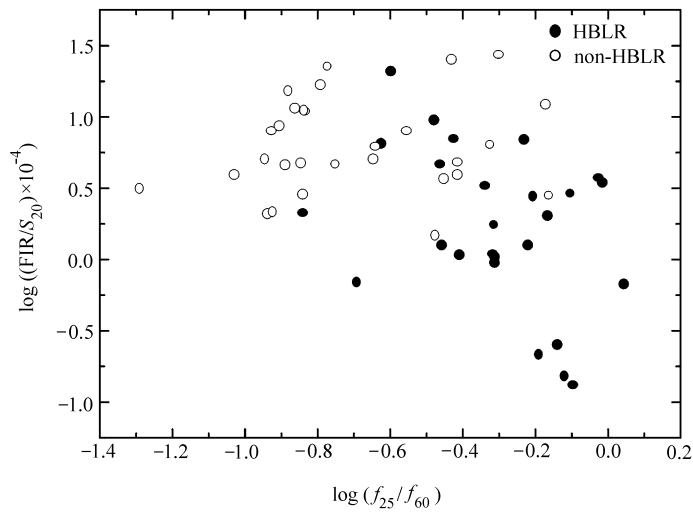
Fig. 5　Flux ratio of FIR/S_{20} versus f_{25}/f_{60} for the two types of Sy2s.

3.3　S_{20} versus FIR

It is well known that a tight correlation exists between the radio and far-IR (FIR) emissions for normal, starburst, and Seyfert galaxies (Helou et al. 1985). More recently, Ji et al. (2000)

have studied the radio−FIR relation of LINERs, and found that AGN and starburst-supported LINERs can be distinguished on this diagram. An analogous plot of the radio−FIR relation between HBLR and non-HBLR Sy2s was given by Gu et al. (2001) which showed that the HBLR Sy2s are located mostly above the standard starburst correlation, thus indicating the existence of an additional contribution to the radio emission due to AGN activities. The non-HBLR Sy2s followed more closely the "normal" starburst relation, implying that in these objects the starburst component might dominate both the FIR and the radio emissions. In Figure 6 we also show the plot of the radio−FIR relation for our sample. It appears that the non-HBLR Sy2s are more like starburst galaxies in regard of the radio and FIR emissions.
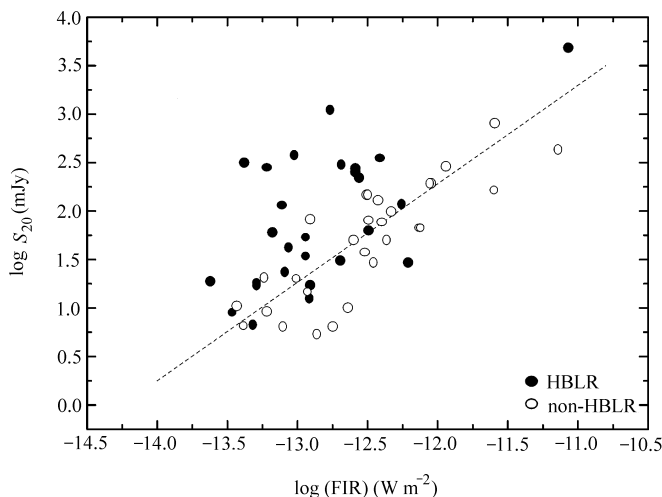
Fig. 6   Distribution of FIR and radio fluxes for the Sy2s in spectropolarimetry. The dashed line is the fit for normal and starburst galaxies from Helou et al. (1985).

4   DISCUSSION

Our first finding that star-formation activity is stronger in the Sy2s without HBLR than those with HBLR is consistent with both the results of Alexander (2001) and Gu et al. (2001), and the finding that the Sy2s without HBLR usually show a stronger galactic emission and a weaker active core emission. Moreover, our larger sample confirms that the Sy2s with HBLR have a high [OIII]λ5007Å intensity as regards both the equivalent width and the emission line ratio. This indicates that the detectability of HBLR is mainly dependent on the luminosity ratio of the active core to the host galaxy (Lumsden et al. 2001). Also, the plot of the radio versus FIR flux shows that the non-HBLR Sy2s are more tightly related to starburst galaxies. The result suggests that the star-formation component plays a significant role in these objects. On the other hand, the fact that the absorbing column density is nearly indistinguishable between the two types of Sy2s, (though the $N_{\rm H}$ in the non-HBLR Sy2s is marginally higher,) excludes a direct interpretation based on the inclination of the torus to the line of sight. The explanations given by Alexander (2001), Gu et al. (2001), and Lumsden et al. (2001) are applicable, but

the interpretation that the non-HBLR Sy2s are "pure" Seyfert 2s with weak or absent BLR is also possible (Tran 2001). Here we argue that the detectability of HBLR may indicate an evolutionary connection, with the non-HBLR Sy2s being found in younger phases.

As mentioned above, both the mid-IR color f_{25}/f_{60} and [OIII]λ5007Å line emission show that the Seyfert 2s with HBLR exhibit a higher AGN activity than those without HBLR. Moreover, the indicators, f_{60}/f_{100} and $L_{\mathrm{FIR}}/L_{\mathrm{B}}$, reveal that the non-HBLR Sy2s have a stronger star-formation activity in the circumnuclear regions. In other words, the Sy2s with a lower core activity have a higher star-formation contribution, while the Sy2s with a lower star-formation activity present a higher AGN contribution. As discussed by Lei et al. (2000), this finding suggests a possible connection between the host galaxies and nuclear activity, and the Seyfert 2s with stronger AGN and weaker star-formation activities, the HBLR Sy2s, might be at a later evolutionary stage. This evolution might also indicate the suggestion offered by de Carvalho & Coziol (1999) that the massive black holes in Sy2s, compete with starbursts for the inflowing gas.

Another indication of the evolutionary connection is the radio–FIR relation. Figure 6 clearly shows that the Sy2s with HBLR are located in a region of higher radio flux with respect to the starburst/normal galaxies, while the non-HBLR Sy2s closely follow the starburst correlation. Furthermore, considering the dominance of starbursts in some Sy2s, several authors suggested that the non-detectability of HBLR is because that the broad-line region is very weak or absent. Indeed, for some Sy2s without HBLR we know that the BLR does exist from hard X-ray observations (Lumsden et al. 2001). However, there are some non-HBLR Sy2s without any report of hard X-ray emission. These objects are the best candidates for the Seyfert 2s with absent BLR if their starburst components are also apparent, and there are also theoretical reasons to believe that intrinsic AGNs may lack BLR (Nicastro 2000; Collin & Huré 2001). In most cool Seyfert 2s the BLR is weak or absent, having just formed or having not yet had sufficient time to form. The situation is similar to the non-existence of quasars in most "cold" ULIRGs (Tran et al. 1999). Relative to Sy2s with HBLR, these cool, non-HBLR Sy2s may be at an earlier evolutionary stage.

In addition, Gu et al. (2001) found that the Sy2s without HBLR display a marginally larger absorbing column density, which is attributed to 100 pc-scale dusty structures, at least in some cases. These dust lanes, with scales large compared to the torus, provide better conditions for circumnuclear star-formation activities, and also for hiding the mirror which reflects the broad lines. In contrast, none of the Sy2s with HBLR show the 100 pc-scale dust lane feature. This may imply that the competition between massive black holes and starbursts for the inflowing gas is at a late stage. The existence of circumnuclear dust lanes might be at a relatively early phase. Thus, the feature of the 100 pc-scale dust lanes in the non-HBLR Sy2s may indicate that this type of Sy2s is at a younger evolutionary system than the type with HBLR.

5 CONCLUSIONS

In this paper, we collected 75 Seyfert 2 galaxies with spectropolarimetric observation data, comprising 38 with HBLR and 37 without HBLR. For these objects, we compared their star-formation components by means of two indicators, f_{60}/f_{100} and $L_{\mathrm{FIR}}/L_{\mathrm{B}}$, and found that, statistically, the non-HBLR Sy2s display a higher star-formation activity than the HBLR Sy2s. We also confirmed the previous finding that the Sy2s with HBLR have stronger [OIII]λ5007Å emissions and FIR-radio flux ratios, indicating a higher luminosity ratio of the core to the host

galaxy. Furthermore, we plotted the radio−FIR relation for our larger sample and obtained the same result as Gu et al. (2001), that the Sy2s without HBLR follow more tightly the radio versus FIR relation of starburst galaxies, at while the HBLR Sy2s tend to spread towards higher core radio emissions.

Based on the results previously found by other authors and on the result obtained in this paper, we argue that the non-HBLR Sy2s may be at an earlier evolutionary stage than the HBLR Sy2s. The most significant evidence is that, compared to the HBLR Sy2s, the non-HBLR Sy2s show a weaker AGN activity component and a stronger star-formation component. Furthermore, the same radio−FIR relation for the non-HBLR Sy2s as starburst galaxies implies that the properties of the non-HBLR Sy2s are more similar to those of starburst galaxies. In addition, the existence of circumnuclear dust lanes in some non-HBLR Sy2s provides better conditions for star-formation activities. Consequently, the Sy2s without HBLR are probably younger Sy2s.

References

Alexander D. M., 2001, MNRAS, 320L, 15
Alonso-Herrero A., Ward M. J., Kotilainen K., 1997, MNRAS, 288, 977
Antonucci R., Miller J. S., 1985, ApJ, 297, 621
Awaki H., Ueno S., Taniguchi Y. et al., 2000, ApJ, 542, 175
Bassani L., Dadina M., Maiolino R. et al., 1999, ApJS, 121, 473
Clavel J., et al., 2000, A&A, 357, 839
Collin S., Huré J., 2001, A&A, 372, 50
de Carvalho R. R., Coziol R., 1999, AJ, 117, 1657
de Grijp M. H. K., Keel W. C., Miley G. K. et al., 1992, A&AS, 96, 389
Dahari O., de Robertis M. M., 1988, ApJS, 67, 249
Gonalves A. C., Véron-Cetty M.-P., Vron P., 1999, A&AS, 135, 437
Granato G. L., Danese L., Franceschini A., 1997, ApJ, 486, 147
Gu Q., Maiolino R., Dultzin-Hacyan D., 2001, A&A, 366, 765
Heisler C. A., Lumsden S. L., Bailey J. A., 1997, Nature, 385, 700
Helou G., Soifer B. T., Rowan-Robinson M., 1985, ApJ, 298L, 7
Ho L. C., Filippenko A. V., Sargent W. L. W., 1997, ApJS, 112, 315
Huang J. H., Gu Q. S., Su H. T. et al., 1996, A&A, 313, 13
Hunt L. K., Malkan M. A., 1999, ApJ, 516, 660
Lei S. J., Huang J. H., Zhang W. et al., 2000, ApJ, 544, L31
Ji L., Chen Y., Huang J. H. et al., 2000, A&A, 355, 922
Keel W. C., 1993, AJ, 106, 1771
Lumsden S. L., Heisler C. A., Bailey J. A. et al., 2001, MNRAS, 327, 459
Maiolino R., 2000, In: G. Malaguti, G. G. C. Palumbo, N. White, eds., X-ray Astronomy 1999, in press (astro-ph/0007473)
Matt G., 2000, A&A, 355, L31
Moran E. C., Barth A. J., Kay L. E., Filippenko A. V., 2000, ApJ, 540, L73

Nicastro F., 2000, ApJ, 530, L65

Risaliti G., Maiolino R., Salvati M., 1999, ApJ, 522, 157

Rodriguez Espinosa J. M., Pérez Garcia A. M., 1997, ApJ, 487, L33

Strauss M. A., Davis M., Yahil A., Huchra J. P., 1990, ApJ, 361, 49

Tran H. D., 1995, ApJ, 440, 565

Tran H. D., Brotherton M. S., Stanford S. A. et al., 1999, ApJ, 516, 85

Tran H. D., 2001, ApJ, 554, L19

Turner T. J., George I. M., Nandra K., Mushotzky R. F., 1997, ApJ, 488, 164

Strauss M. A., Huchra J. P., Davis M. et al., 1992, ApJS, 83, 29

Véron-Cetty M. P., Véron P., 2000a, A&AR, 10, 81

Véron-Cetty M. P., Véron P., A Catalogue of Quasars and Active Galactic Nuclei, (2000), 9th ed.
  (ESO, Garching near Munich)

Whittle M., 1992, ApJS, 79, 49